Evaluation of Reduced-Rank, Adaptive Matched Field Processing Algorithms for Passive Sonar Detection in a Shallow-Water Environment*

Nigel Lee, Lisa M. Zurk, and James Ward
MIT Lincoln Laboratory
Lexington, MA
nigel@ll.mit.edu, zurk@ll.mit.edu, jward@ll.mit.edu

Abstract

This paper evaluates the performance of several reduced-rank, adaptive matched field processing (AMFP) algorithms for passive sonar detection in a shallow-water environment. Effective rank reduction improves the stability of adaptive beamformer weight calculation when the number of available snapshots is limited. Here, rank-reduction techniques with various criteria for subspace selection are evaluated within a common framework and compared to the full-rank conventional and minimum-variance (MVDR) beamformers. Results from real data demonstrate that rank reduction, properly applied, can improve AMFP detection performance in practical system implementations.

1 Background

Matched field processing (MFP) has been widely proposed as an array processing technique for passive sonar detection and localization with vertical line arrays in littoral environments. MFP exploits the coherent multipath of signals propagating in the ocean waveguide by incorporating propagation physics into the computation of "replica" (steering) vectors from which beamformer weights are derived, resulting in accurate source localization in range, depth, and bearing.

In the results presented here, an adiabatic approximation is used to compute range-dependent replica vectors using output from the KRAKEN normal mode propagation model [8]. For an array with N elements, each $N \times 1$ replica vector $\vec{v}$ is normalized such that $\vec{v}^H \vec{v} = N$. The MFP weight vector $\vec{w}$ is derived from the replica vector $\vec{v}$, and the MFP output power is then computed as

$$\mathrm{P_{MFP}}(\theta) = \vec{w}^H(\theta)\hat{\mathbf{K}}\vec{w}(\theta)\,, \tag{1}$$

where θ represents the parameters of the MFP search space, usually range and depth, and where

$$\hat{\mathbf{K}} = \frac{1}{L}\sum_{l=1}^{L} x_l x_l^H \tag{2}$$

is the sample covariance matrix, computed as a summation of $N \times 1$ data snapshots x_l. The spatial variable θ will be omitted for ease of notation in the development below, but it is always assumed implicitly.

The conventional, or Bartlett, MFP processor (**CMFP**) computes a weight vector that is a scaled version of the replica vector, $\vec{w}_c = \vec{v}/N$, where the scaling ensures the unity gain constraint, $\vec{w}^H\vec{v} = 1$. CMFP detects strong sources well and is robust to mismatch, but it suffers from high sidelobes that can obscure detection and degrade localization accuracy, especially in the presence of strong interferers.

The standard adaptive MFP (AMFP) processor, called **minimum-variance, distortionless response (MVDR)**, computes a data-dependent weight vector that is a function of both the replica vector and the sample covariance matrix:

$$\vec{w}_m = \frac{\hat{\mathbf{K}}^{-1}\vec{v}}{\vec{v}^H\hat{\mathbf{K}}^{-1}\vec{v}}\,. \tag{3}$$

The MVDR output is then computed as

$$\mathrm{P_{MVDR}} = \vec{w}_m^H\hat{\mathbf{K}}\vec{w}_m = \left\{\vec{v}^H\hat{\mathbf{K}}^{-1}\vec{v}\right\}^{-1}\,. \tag{4}$$

Compared to CMFP, MVDR provides significant interference rejection and sidelobe suppression and thus much better source localization, with comparable detection performance in the absence of mismatch. However, computation of the MVDR weights $\vec{w}_m$ is very sensitive to signal mismatch because of the dependence on $\hat{\mathbf{K}}$, which may contain

*This work was sponsored by DARPA-TTO under Air Force contract F19628-95-C-0002. Opinions, interpretations, conclusions, and recommendations are those of the authors and are not necessarily endorsed by the United States Air Force.

0-7803-5700-0/99/$10.00©1999 IEEE

small eigenvalues that disproportionately affect the MVDR output (4).

One method of improving the robustness of MVDR processing is to apply *diagonal loading* to the weight computation:

$$\vec{w}_{m_{DL}} = \frac{(\hat{\mathbf{K}} + \sigma_d^2\mathbf{I})^{-1}\vec{v}}{\vec{v}^H(\hat{\mathbf{K}} + \sigma_d^2\mathbf{I})^{-1}\vec{v}}, \quad (5)$$

where the *load level* σ_d^2 is chosen to satisfy some white noise gain constraint [3]. The diagonally-loaded MVDR output is then computed as in (4), with $\vec{w}_{m_{DL}}$ replacing $\vec{w}_m$.

Rank reduction is another technique for improving MVDR robustness. Under the assumption of Gaussian statistics for $\hat{\mathbf{K}}$, Reed *et al.* [9] showed that the SINR power loss ρ incurred by using the sample covariance matrix $\hat{\mathbf{K}}$ to compute the MVDR output instead of the true data covariance matrix $\mathbf{K}$ has expected value

$$\mathcal{E}(\rho) = (L - N + 2)/(L + 1), \quad (6)$$

where L and N are defined as above. In practice, the number of snapshots L available to compute $\hat{\mathbf{K}}$ is limited by nonstationarity in the data (e.g., due to source motion, time-varying background noise, etc.); however, SINR losses of 3 dB or more are incurred in (6) if $L < 2N$. Rank reduction addresses this "limited snapshot" problem by replacing $\hat{\mathbf{K}}$ with a rank-P approximation $\mathbf{K}_R$ ($P \ll N$) in (3), effectively replacing N with P in (6). In the following, several algorithms for determining the reduced-rank approximation $\mathbf{K}_R$ are detailed, and the resulting reduced-rank MFP algorithms are evaluated for a common data set, with the full-rank CMFP and MVDR serving as performance baselines.

2 Rank Reduction Algorithms

The first three rank reduction algorithms examined here can be loosely classified as eigenvector (EV) filtering algorithms. To understand them, first let the eigenvector decomposition of $\hat{\mathbf{K}}$ be given as

$$\hat{\mathbf{K}} = \mathbf{U}\mathbf{\Sigma}\mathbf{U}^H = \sum_{i=1}^{N} \sigma_i^2 \vec{u}_i \vec{u}_i^H, \quad (7)$$

where $\mathbf{U} = [\ \vec{u}_1 \quad \vec{u}_2 \quad \ldots \quad \vec{u}_N\ ]$ is an orthogonal matrix whose columns are comprised of the eigenvectors $\vec{u}_i$ of $\mathbf{K}$ ($\vec{u}_i^H\vec{u}_i = 1\ \forall i$) and $\mathbf{\Sigma} = diag(\sigma_1^2, \sigma_2^2, \ldots, \sigma_N^2)$ is a diagonal matrix whose diagonal elements are comprised of the eigenvalues σ_i^2 of $\mathbf{K}$ (usually ordered such that $\sigma_1^2 \geq \sigma_2^2 \geq \ldots \geq \sigma_N^2$).

The eigenvector filtering algorithms approximate $\hat{\mathbf{K}}$ with a rank-P approximation $\mathbf{K}_R$, where

$$\mathbf{K}_R = \mathbf{U}\mathbf{\Sigma}_R\mathbf{U}^H = \sum_{i=1}^{P} \sigma_{R_i}^2 \vec{u}_{R_i} \vec{u}_{R_i}^H, \quad (8)$$

and $\mathbf{\Sigma}_R = diag(\sigma_{R_1}^2, \sigma_{R_2}^2, \ldots, \sigma_{R_P}^2, 0, \ldots, 0)$. Note that $N - P$ eigenvalues have been "zeroed out" (filtered) and the remaining P eigenvalues have been re-indexed to be the first P eigenvalues of $\mathbf{\Sigma}_R$ (so that there is an implicit reordering of the columns of $\mathbf{U}$ in (8) as well).

The three eigenvector filtering algorithms are distinguished by the criterion used to select which eigenvalue/eigenvector pairs to keep for $\mathbf{K}_R$. The **reduced minimum variance (RMV)** algorithm [2, 7] retains the P largest eigenvalues (and corresponding eigenvectors) of $\hat{\mathbf{K}}$. The **signal coherence (SC)** algorithm [5] selects the eigenvectors (and corresponding eigenvalues) that have large enough correlation with the replica vector $\vec{v}$, i.e.,

$$\left|\vec{u}_i^H\vec{v}\right|^2 \geq \gamma\left|\vec{v}\right|^2, \quad (9)$$

where γ is some scalar constant; setting $\gamma = 0.5$, for example, retains those eigenvectors whose correlation is within 3 dB of the maximum. If, for a given replica vector, no eigenvectors satisfy (9), the SC algorithm uses the full-rank MVDR output (4). Note that the criterion (9) is such that both the reduced-rank subspace and the dimension P of the subspace *will vary* with spatial parameters θ in the SC algorithm. The **direct form (DF)** algorithm [10] retains the P eigenvalue/eigenvector pairs that maximize, for each $\vec{v}$, the ratio

$$\left|\vec{u}_i^H\vec{v}\right|^2 / \sigma_i^2. \quad (10)$$

The DF criterion again is such that the reduced-rank subspace varies with spatial parameters θ, although the dimension P is fixed for all θ. The DF criterion selects the subspace that minimizes MVDR output power over all P-dimensional eigenvector bases, which should maximize output SINR under ideal conditions. Practically, however, the DF criterion needs to be applied in conjuction with diagonal loading to reduce the sensitivity of (10) to small eigenvalues during subspace selection.

Once $\mathbf{K}_R$ is determined, the reduced-rank MVDR weight vector $\vec{w}_R$ is computed as

$$\vec{w}_R = \frac{\mathbf{K}_R^{-1}\vec{v}}{\vec{v}^H\mathbf{K}_R^{-1}\vec{v}}. \quad (11)$$

and the reduced-rank MVDR output is computed as

$$\mathrm{P}_{\mathrm{MVDR_{RR}}} = \vec{w}_R^H\hat{\mathbf{K}}\vec{w}_R. \quad (12)$$

Note that the reduced-rank covariance $\mathbf{K}_R$ is used only for the weight computation in (11) and the original (full-rank) sample covariance $\hat{\mathbf{K}}$ is still used in (12). However, for the EV filtering algorithms, the expression in (12) reduces to

$$\mathrm{P}_{\mathrm{MVDR_{RR}}} = \left\{\vec{v}^H\mathbf{K}_R^{-1}\vec{v}\right\}^{-1} \quad (13)$$

$$= \left\{\sum_{i=1}^{P} \sigma_{R_i}^{-2}\left|\vec{u}_{R_i}^H\vec{v}\right|^2\right\}^{-1}. \quad (14)$$

A fourth eigenvector-based algorithm that takes a different approach to rank reduction is the **dominant mode rejection (DMR)** algorithm [6]. In the DMR algorithm, $\mathbf{K}_R$ is constructed by retaining the largest P eigenvalues of $\hat{\mathbf{K}}$ (much like the RMV algorithm), but the remaining N-P small eigenvalues are *averaged* instead of *filtered*. Thus, $\mathbf{K}_R = \mathbf{U}\mathbf{\Sigma}_R\mathbf{U}^H$, where $\mathbf{\Sigma}_R = diag(\sigma_1^2, \sigma_2^2, \ldots, \sigma_P^2, \alpha, \alpha, \ldots, \alpha)$ and

$$\alpha = \frac{1}{N-P}\sum_{i=P+1}^{N}\sigma_i^2 . \tag{15}$$

The reduced-rank MVDR weight vector $\vec{w}_R$ is then computed as in (11) and the reduced-rank MVDR output $\mathrm{P}_{\mathrm{MVDR_{RR}}}$ as in (12); however, simplification to (14) is not possible because DMR is not a reduced-dimension algorithm. The DMR algorithm is such that adaptive nulling still occurs in (11) in the directions of the dominant eigenvectors (thus the name of the algorithm) while nulling is reduced in other directions.

Cox and Pitre [4] showed that for DMR applied in combination with diagonal loading, the reduced-rank MVDR weight vector is given by

$$\vec{w}_R = \frac{\vec{v} - \sum_{i=1}^{P}\beta_i(\vec{u}_i^H\vec{v})\vec{u}_i}{N - \sum_{i=1}^{P}\beta_i\left|\vec{u}_i^H\vec{v}\right|^2}, \tag{16}$$

where $\beta_i = (\sigma_i^2 - \alpha)/(\sigma_i^2 + \sigma_d^2)$ and σ_d^2 is the diagonal load level. The same authors also suggest a modification for mismatch protection, so that off-boresight mainlobe signals are not suppressed. This is implemented by imposing the SC constraint (9) and *deleting* the eigenvectors having large correlations with the replica vector from the weight computation in (16).

The fifth rank-reduction algorithm examined in this paper is the **modal decomposition (MD)** algorithm [11]. Here, both data and replica vectors are transformed from phone space into mode space:

$$\vec{v}_m = \mathbf{T}_m\vec{v} \tag{17}$$

$$\mathbf{K}_m = \mathbf{T}_m\mathbf{K}\mathbf{T}_m^H , \tag{18}$$

where $\vec{v}_m$ is the "mode replica" vector, $\mathbf{K}_m$ is the modal covariance matrix, and $\mathbf{T}_m = (\mathbf{Q}^H\mathbf{Q})^{-1}\mathbf{Q}^H$ is the modal transformation matrix derived from the mode space matrix $\mathbf{Q}$, whose columns are mode functions sampled at the depths of the vertical line array, with array tilt taken into account.

Mode filtering then takes place in the mode domain, with $\mathbf{K}_R$ computed by retaining P rows and columns of $\mathbf{K}_m$ and "zeroing" the other N-P rows and columns. The advantage of transforming into mode domain is that the mode functions have an easily understood physical meaning. For example, retaining the P low-order modes filters out most surface energy, because only higher-order modes are excited near the surface. Once $\mathbf{K}_R$ has been computed, the reduced-rank MVDR weight vector is computed in the mode domain as

$$\vec{w}_{m_R} = \frac{\mathbf{K}_R^{-1}\vec{v}_m}{\vec{v}_m^H\mathbf{K}_R^{-1}\vec{v}_m}, \tag{19}$$

and reduced-rank "matched mode" power is given by

$$\mathrm{P}_{\mathrm{MODE_{RR}}} = \vec{w}_{m_R}^H\hat{\mathbf{K}}_m\vec{w}_{m_R} . \tag{20}$$

Note that the mode functions in $\mathbf{Q}$ are not orthogonal unless the vertical line array spans the water column. Thus, the mode transformation $\mathbf{T}_m$ may not be orthogonal, and this needs to be accounted for in comparing matched mode output in (20) to matched field output in (1). For the data presented here, however, the vertical line arrays span most of the water column and the modes vectors are approximately orthogonal.

3 Comparison of Reduced-Rank AMFP Algorithms for Real Data

The data analyzed here was collected during the Santa Barbara Channel Experiment (SBCX), conducted in April 1998 in the 100 to 300m-deep waters of the Santa Barbara channel. During SBCX, data was collected using a 150-hydrophone "full-field processing" (FFP) array comprised of five vertical line arrays (VLA's) of 30 phones each, with each VLA moored at the vertices of a 200m-diameter pentagon. The volumetric nature of the FFP array enabled accurate source detection and accurate localization in range, depth, and bearing.

One of the acoustic sources deployed during SBCX was a J15-3 transducer that was towed by a research vessel, the Acoustic Explorer (AX). The transducer was used to generate a comb signal of 12 tones at approximately 159 dB re 1 μPa/Hz source level. The results shown here were generated from 100s of time series data (during which the comb signal was on), passed through an FFT with a nonoverlapping, 1s Hanning window and processed at the comb frequency of 235 Hz. Beamforming was done using one VLA of 30 phones (N=30). Note that L=100 snapshots were available for time-averaged covariance estimation if all 100s of data were used; however, the range of the AX during this data segment was less than 2km, so MFP processing using all 100s of data was affected by mismatch due to the motion of the AX.

In Example 1, all 100s of data were processed. The mean position of the AX during this time was 1.7km range and 28m depth. Input signal level was 99.8 dB, computed by

taking an average of the FFT bin corresponding to 235 Hz over the $100s$ time interval. The input noise level was 91.8 dB, measured from neighboring frequency bins in the FFT. Thus, the input SNR was $\approx$8 dB. Figure 1 shows the range-depth ambiguity surfaces of eight MFP processors for Example 1: full-rank CMFP; full-rank MVDR with diagonal loading (MVDR-DL); RMV with P=10; SC with γ=0.5; DF with P=10 and diagonal loading (DF-DL); DMR with P=10, diagonal loading, and mismatch protection (γ=0.5); and MD with P=10 and P=15 low-order modes retained.

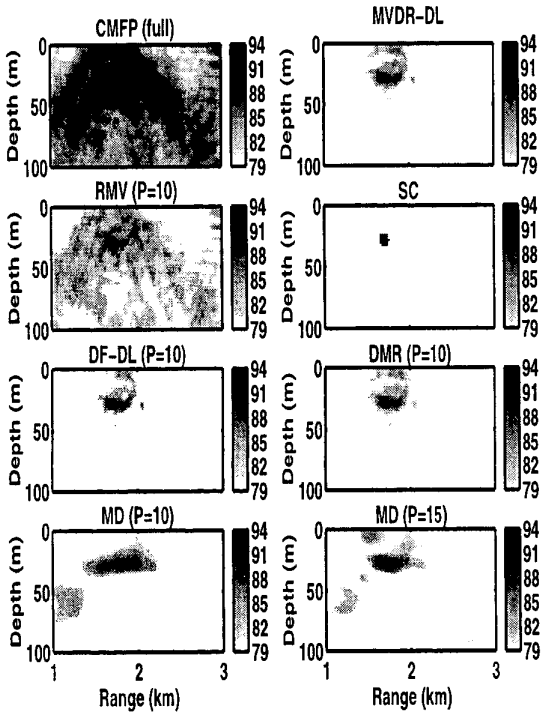

Figure 1. MFP ambiguity surfaces from 100s of data. Gray scale units are dB re 1 μPa/Hz.

For the full-rank processors, CMFP has a strong peak at the source location but the expected high sidelobes, while the adaptive sidelobe cancellation in MVDR-DL results in much better localization. However, note that the source peak is "smeared" even for MVDR-DL due to source motion during the $100s$ time interval. The best source localization of any processor is provided by SC, which works well for fairly high SNR's; setting $\gamma = 0.5$ in (9) produces a subspace of rank-1 in a local neighborhood of the source and rank-0 (with full adaptive cancellation) elsewhere. RMV produces results between that of CMFP and MVDR-DL, because adaptive cancellation occurs only among the eigenvectors that have been retained, which always correspond to the largest 10 eigenvalues; this is a weakness of RMV, because the appropriate dimension of the reduced-rank subspace is not necessarily constant across the ambiguity surface. DF-DL provides the highest output SNR of any processor, at the cost of greater mismatch loss at the source (both as a result of the DF criterion). DMR produces nearly the same results as MVDR-DL, with differences due to the averaging procedure of (15). Finally, MD provides good rejection of surface energy, as intended, but performance varies with the number of modes retained. The results are summarized in Table 1, which lists output signal level, computed as the MFP output at range $1.7km$ and depth $28m$; output noise, computed as the lower quartile of MFP power over the entire ambiguity surface; and output SNR, the ratio of the two.

Process	Signal Out (dB)	Noise Out (dB)	SNR Out (dB)
CMFP	94.2	84.3	9.9
MVDR-DL	91.9	70.5	21.4
RMV	92.7	79.1	13.6
SC	94.0	69.3	24.7
DF-DL	92.5	66.3	26.2
DMR	96.3	72.9	23.4
MD-10	90.8	72.6	18.2
MD-15	92.3	72.5	19.8

Table 1. MFP results for Example 1. Signal In=99.8 dB, Noise In=91.8 dB, SNR In=8 dB.

Example 2 processes $21s$ of data in the middle of the original $100s$ time segment. For Example 2, the input signal was again 99.8 dB and the input noise was computed to be 89.2 dB, so the input SNR was 10.6 dB. Figure 2 shows the range-depth ambiguity surfaces of the eight MFP processors for Example 2.

Note first that with 21 snapshots, the 30 $\times$ 30 sample covariance $\mathbf{K}$ is not full rank, and its inverse (computed using SVD-based approximation) does not produce accurate adaptive nulling. Thus, MVDR-DL performs poorly. Of the reduced-rank algorithms, RMV and MD still suffer from potentially poor performance due to improper subspace size. However, the best reduced-rank techniques – SC, DF, and DMR – perform even better than in Example 1, because there is less mismatch loss due to motion and better source localization for the shorter time period. Example 2, then, demonstrates the full advantage of applying rank reduction to AMFP processing: reduced-rank weight vectors are computed accurately with a severely limited number of snapshots (L=21), as rank reduction from N=30 to P=10 (or lower) enables $L \geq 2P$. Table 2 summarizes the results for Example 2.

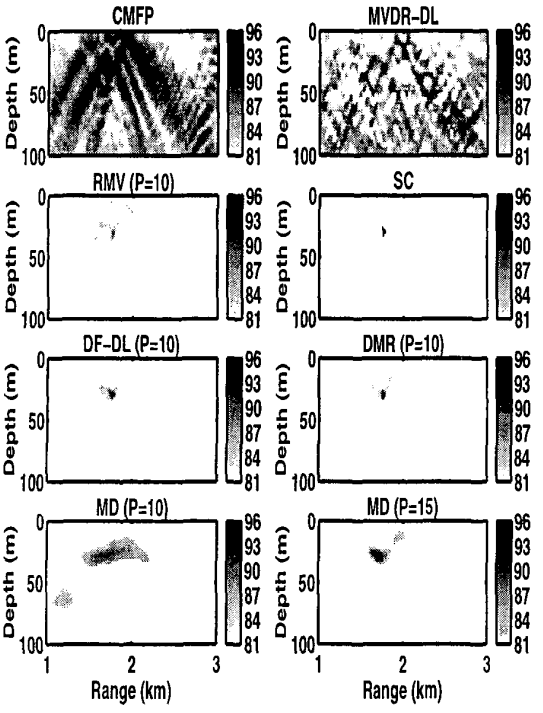

Figure 2. MFP ambiguity surfaces from 21s of data. Gray scale units are dB re 1 μPa/Hz.

4 Discussion

This paper examined the performance of several reduced-rank AMFP algorithms on a common set of data. It was demonstrated that the most effective rank-reduction techniques – the signal coherence, direct form, and dominant mode rejection algorithms – improve the stability of adaptive weight calculation (and therefore improve AMFP detection performance) when the number of available snapshots is limited, a very important scenario for passive sonar detection in shallow water. It should be noted that the examples processed here had fairly high SNR's (8-10 dB input SNR), and it remains to be shown how the various rank reduction algorithms will perform in low-SNR environments, where distinctions among the algorithms should be more apparent. How performance varies with subspace rank is also an open question. Finally, analysis of data with strong surface interferers is necessary to demonstrate the true utility of the modal decomposition algorithm, where rank reduction with the physically-based modal basis can be applied easily. All of these are topics for further study.

Process	Signal Out (dB)	Noise Out (dB)	SNR Out (dB)
CMFP	96.6	82.7	13.9
MVDR-DL	93.0	79.1	13.9
RMV	88.5	73.7	14.8
SC	96.5	69.6	26.9
DF-DL	90.9	57.5	33.4
DMR	98.5	67.3	31.2
MD-10	90.4	68.8	21.6
MD-15	92.0	67.9	24.1

Table 2. MFP results for Example 2. Signal In=99.8 dB, Noise In=89.2 dB, SNR In=10.6 dB.

References

[1] A. Baggeroer, W. Kuperman, and P. Mikhalevsky. An overview of matched field methods of ocean acoustics. *IEEE Journal of Oceanic Engineering*, 18(4):401–424, Oct. 1993.

[2] C. Byrne et al. A stable data-adaptive method for matched-field array processing in acoustic waveguides. *Journal of the Acoustical Society of America*, 87(6):2493–2502, 1990.

[3] H. Cox. Robust adaptive beamforming. *IEEE Transactions on Acoustics, Speech, and Signal Processing*, 35(10):1365–1376, Oct. 1987.

[4] H. Cox and R. Pitre. Robust DMR and multi-rate adaptive beamforming. In *1997 31st Asilomar Conference*, pages 920–924, 1997.

[5] Y. Lee et al. Robust adaptive matched-field-processing. In *Proceedings of the Conference on Oceans '93*, pages 387–392, 1993.

[6] N. Owsley. Sonar array processing. In S. Haykin, editor, *Array Signal Processing*. Prentice-Hall, New Jersey, 1985.

[7] J. Ozard, G. Brooke, and P. Brouwer. Improving performance for matched field processing with a minimum variance beamformer. *Journal of the Acoustical Society of America*, 91(1):141–150, 1992.

[8] M. Porter. The KRAKEN normal mode program. Technical Report SM-245, SACLANT Undersea Research Centre, 1991.

[9] I. Reed, J. Mallett, and L. Brennan. Rapid convergence rate of adaptive arrays. *IEEE Transactions on Aerospace Electronic Systems*, 10(6):853–863, 1974.

[10] J. Ward, A. Baggeroer, and L. Zurk. Rapidly adaptive matched field processing for nonstationary environments. In *1998 Adaptive Sensor Array Processing Workshop*, Lexington, MA, Mar. 1998.

[11] T. Yang. Effectiveness of mode filtering: A comparison of matched-field and matched-mode processing. *Journal of the Acoustical Society of America*, 87(5):2072–2084, 1990.